Efficient Neuro-Fuzzy Damage Severity Estimation in an Experimental Wind Turbine Blade Using the Fukunaga-Koontz Transform of Vibration Signal Correlations

Simon HOELL, Piotr OMENZETTER

The LRF Centre for Safety and Reliability Engineering
The University of Aberdeen, AB24 3UE, Aberdeen, UK
r01sh13@abdn.ac.uk, piotr.omenzetter@abdn.ac.uk

Abstract

Potential energy outputs of wind turbines (WTs) are subject to continuous enhancements due to increasing demands for carbon neutral energy. The use of novel composite materials facilitates erections of ever larger WTs, which capture more energy by using longer WT blades (WTBs) with reduced weight. However, higher flexibilities and lower buckling capacities of these WTBs adversely affect long-term safety and reliability of WTs and, with it, energy production costs. This can be counteracted with the help of efficient structural health monitoring (SHM). The present study shows a novel methodology for vibration-based structural damage detection and severity estimation in WTBs. First, correlations of vibrational response signals are extracted as initial damage sensitive features (DSFs). Second, the Fukunaga-Koontz transform, an extension of the better-known Karhunen-Loéve expansion, is applied for extracting secondary DSFs with improved damage sensitivities. Third, univariate rankings of both DSFs are separately created with respect to the area under the receiver operating characteristic curve. Then, structural damage detection and severity estimation is performed with the help of hierarchical adaptive neuro-fuzzy inference systems, where the hierarchical structure allows accounting for the ranking information. The method is applied to laboratory experimental data from a small WTB exited by an air stream produced by a household fan. Damage severity estimation is studied by attaching different small masses as non-destructive damage scenarios. The results demonstrate that the proposed methodology enables to detect and estimate accurately the severity of the simulated damage. Furthermore, the advantages of using transformed DSFs are shown. This is promising for future developments of vibration-based SHM to facilitate improved safety and reliability of WTs at lower costs.

Keywords: Damage detection, Damage severity estimation, Neural networks, Fuzzy computing, Wind turbines, Time series methods, Fukunaga-Koontz transform

1. INTRODUCTION

Recent international commitments for achieving carbon neutrality in the present century pave the way for further advancements in wind energy [1]. To satisfy increasing energy production demands, potential energy outputs are continuously enhanced by erections of ever larger wind turbines (WTs). These developments can be facilitated by the use of novel composite materials for manufacturing WT blades (WTBs) with reduced weight. However, the long-term safety and reliability of WTs are adversely affected by higher flexibilities and lower buckling capacities of these WTBs [2,3]. Additionally, international standards and guidelines

recommend rigidly defined physical inspection intervals for examining the structural state of WTs. The operation and maintenance costs can make up to 20% of the total wind energy production costs [4]. The development of effective structural health monitoring (SHM) techniques can help to reduce these costs because onsite inspections efforts can be limited and maintenance actions can be scheduled according to the true structural state and condition.

Several sensing technologies based on different physical principles are available for structural damage detection in WTBs [5], but the majority of these techniques are not applicable for continuous monitoring tasks of large structures in harsh environments. Structural vibrations resulting from ambient excitations are affected by changes in stiffness, mass or energy dissipation mechanisms of a structure, which are often result from damage. The development of vibration-based SHM techniques receives considerable attention, where the availability of mature and cost effective sensing technology facilitates progress. Furthermore, instrumentation costs are competitive because these global vibrations can encompass the entire structure due to long wavelengths and low damping and therefore require limited numbers of sensors to measure. Different damage sensitive features (DSFs) can be extracted from vibration response signals, such as modal parameters, parametric time series model coefficients, and non-parametric time series representations in frequency, time-frequency and time domains [6]. In this study, initial DSFs are defined as autocorrelation functions (ACFs) – simple and computationally efficient non-parametric time domain representations estimated from acceleration responses.

Decision making about the state of a structure on the basis of DSFs is the next step in the damage detection process. Statistical methods, such as hypothesis testing, are effective for deciding whether a structure is healthy or damaged. However, if obtaining more detailed information about damage, e.g. its severity or location, is desired, then the use of multiple statistical tests is required [7]. These tests are based on prior assumptions of the DSFs' probability distributions and have limited generalization capabilities, which are required for making decisions about unseen damage scenarios. Soft-computing techniques, such as artificial neural networks (ANNs) [8] and support vector machines [9], have the ability to learn complex relationships between inputs, i.e. DSFs, and outputs, e.g. damage severities and locations, directly from data.

The present paper proposes the use of adaptive neuro-fuzzy inference systems (ANFISs) for combined soft-computing based structural damage detection and severity estimation. An ANFIS is a Takagi-Sugeno type fuzzy inference system [10]. It can be represented as ANN with a specific five layer structure, which enables to employ efficient training routines for optimizing model parameters. However, systems with large numbers of inputs, i.e. high dimensional DSFs, can become computationally prohibitive. Therefore, a hierarchical construction scheme is developed using a template ANFIS with two inputs and one output. This enables to account for differently distributed damage sensitivities in multivariate DSFs by incrementally adding hierarchy levels with inputs of decreasing sensitivity. Cross-validation allows then identifying hierarchical ANFISs (HANFISs) with optimal numbers of levels, where accuracy is traded off with the risk of overfitting. However, it can be anticipated that using less but more sensitive DSFs can lead to more accurate, robust and parsimonious models. Therefore, the Fukunaga-Koontz transform (FKT), an extension of the better-known Karhunen-Loéve expansion, of initial DSFs is studied. It uses, in contrast to principal component analysis, two datasets from different classes for estimating a transformation matrix with improved classification performance [11]. In the present case, different classes refer to distinct structural states. The resulting FKT scores, as secondary DSFs, have higher damage sensitivities. For comparing HANFIS models of both DSF types,

the areas under receiver operating characteristic curves (AUCs) are used to create rankings of univariate DSFs. The ranking information is utilized for creating HANFISs with inputs of decreasing sensitivity.

The proposed method is applied to experiments with a small scale WTB made of a glass-fibre composite material. The WTB is excited with the help of a household fan creating a stream of air resembling natural wind. Acceleration responses are measured at the WTB's tip, while damage is introduced non-destructively by attaching small masses at the trailing-edge at approximately 30% of the WTB length from the root. The weight of the masses is used to quantify damage severity.

The paper is structured as follows. First, the theory of the FKT, DSF ranking and HANFIS modelling is introduced. Second, the experimental configuration and the WTB's dynamic characteristics are presented. Then, DSF extraction and HANFIS modelling processes are shown. The results for structural damage detection and severity estimation are additionally discussed. Finally, concluding remarks are presented.

2. THEORY

2.1 Autocorrelation functions and damage sensitive feature

The proposed method aims to detect damage and estimate its severity on the basis of vibrational responses. A discrete acceleration signal, $x[t]$, at a time instant t can be divided into n time series segments, $x_i[t]$, of length N_{samp}. For reducing the effects of varying conditions, zero-mean standardized time series segments, $z_i[t]$, can be obtained by removing the estimated mean, $\hat{\mu}_{x_i}$, and deviding by the estimated standard deviation, $\hat{\sigma}_{x_i}$, where the hat denotes estimate. Then, ACFs, $R_i[\tau]$, at a lag τ can be unbiasedly estimated as [12]:

$$\hat{R}_i[\tau] = \frac{1}{N_{samp} - \tau} \sum_{t=1}^{N_{samp}-\tau} x[t]x[t+\tau] \quad \text{for} \quad \tau = 0,1,2,\ldots,m \tag{1}$$

This enables to define multivariate DSF vectors, $\mathbf{v}_i$, composed of the first m ACF coefficients and a corresponding DSF matrix, $\mathbf{V}$, as:

$$\mathbf{v}_i = \left[\hat{R}_i[1] \quad \hat{R}_i[2] \quad \cdots \quad \hat{R}_i[m] \right]^T \quad \text{and} \quad \mathbf{V} = \left[(\mathbf{v}_1 - \hat{\boldsymbol{\mu}}_v) \quad (\mathbf{v}_2 - \hat{\boldsymbol{\mu}}_v) \quad \cdots \quad (\mathbf{v}_n - \hat{\boldsymbol{\mu}}_v) \right] \tag{2}$$

where T indicates transposition and $\hat{\boldsymbol{\mu}}_v$ is the estimated mean DSF vector. It should be noted that for standardized zero-mean time series segments the ACF is identical with the autocovariance coefficient function, thus the zero lag estimates, $\hat{R}_i[0]$, are ignored because they are constant. This following sections present the theory of the proposed methodology building blocks applied to this DSF type, although other DSFs can be used in a similar way.

2.2 The Fukunaga-Koontz transform

The FKT is an extension of the Karhunen-Loéve expansion, but it does not aim at obtaining an optimal approximation for reconstructing initial datasets with reduced dimensionality. It is rather the best linear approximation of a quadratic classifier [13], which can be obtained in two steps. First, a normalizing transformation matrix is calculated by eigendecomposition of a combined variance-covariance matrix, $\hat{\boldsymbol{\Sigma}}$, as:

$$\hat{\boldsymbol{\Sigma}}_h + \hat{\boldsymbol{\Sigma}}_d = \hat{\boldsymbol{\Sigma}} = \mathbf{U}\mathbf{D}\mathbf{U}^T \tag{3}$$

where $\hat{\boldsymbol{\Sigma}}_h$ and $\hat{\boldsymbol{\Sigma}}_d$ are the estimated variance-covariance matrices of DSFs from the healthy and damaged state, respectively. Matrix $\mathbf{D}$ is diagonal and contains the eigenvalues, λ_i. The corresponding eigenvectors are contained in matrix $\mathbf{U}$. Then, the normalizing transformation

matrix, **P**, can be defined as:

$$\mathbf{P} = \mathbf{U}\mathbf{D}^{-1/2} \tag{4}$$

Using **P**, the variance-covariance matrices can be obtained as as:

$$\tilde{\mathbf{\Sigma}}_h = \mathbf{P}^T \hat{\mathbf{\Sigma}}_h \mathbf{P} \quad \text{and} \quad \tilde{\mathbf{\Sigma}}_d = \mathbf{P}^T \hat{\mathbf{\Sigma}}_d \mathbf{P} \tag{5}$$

where

$$\tilde{\mathbf{\Sigma}}_h + \tilde{\mathbf{\Sigma}}_d = \mathbf{I} \tag{6}$$

and **I** is an identity matrix.

Second, it can be shown that the two transformed variance-covariance matrices share the same eigenspace [11], thus they can be simultaneously diagonalized as:

$$\tilde{\mathbf{\Sigma}}_h = \mathbf{\Phi}\mathbf{\Lambda}_h\mathbf{\Phi}^T \quad \text{and} \quad \tilde{\mathbf{\Sigma}}_d = \mathbf{\Phi}\mathbf{\Lambda}_d\mathbf{\Phi}^T \tag{7}$$

with the common eigenvector matrix $\mathbf{\Phi}$. By substituting Eq. (5)-(7) and eliminating the eigenvector matrices, the following relationship can be obtained:

$$\mathbf{\Lambda}_h + \mathbf{\Lambda}_d = \mathbf{I} \text{ with } \mathbf{\Lambda}_h = \text{diag}\begin{pmatrix} \lambda_{h,1} & \cdots & \lambda_{h,m} \end{pmatrix} \text{ and } \mathbf{\Lambda}_d = \text{diag}\begin{pmatrix} \lambda_{d,1} & \cdots & \lambda_{d,m} \end{pmatrix} \tag{8}$$

Since the symmetric variance-covariance matrices are positive semi-definite and if the eigenvalues for the healthy DSFs, $\lambda_{h,i}$, are arranged in descending order, the eigenvalues of the damaged system, $\lambda_{d,i}$, obey the following:

$$1 \geq \lambda_{d,1} = 1 - \lambda_{h,m} \geq \lambda_{d,2} = 1 - \lambda_{h,m-1} \geq \cdots \geq \lambda_{d,m} = 1 - \lambda_{h,1} \geq 0 \tag{9}$$

The eigenvectors corresponding to the largest eigenvalues of the healthy state are the most important for representing this state, while they are the least important for the other state. Furthermore, this implies that the two states do not share a common important space, but they are most separable in the subspace associated with the eigenvectors of the largest eigenvalues of both states [14]. The combined transformation of the initial DSF matrix, **V**, can now be performed as:

$$\mathbf{S} = \mathbf{\Phi}^T \mathbf{P}^T \mathbf{V} \tag{10}$$

with **S** denoting the FKT scores matrix.

2.3 Damage sensitive feature ranking

The ranking of univariate DSFs is required for creating efficient HANFIS models. Although, the FKT can provide a ranking of the scores depending on the eigenvalues of the both datasets, the same ranking mechanism should be applied to initial and secondary DSFs in order to enable a fair comparison between both DSF types. Receiver operating characteristics (ROCs) allow investigating the performance of a binary classifier without assumptions about probability distributions of DSFs [15]. Additionally, the results are independent of the appropriateness of pre-selected fixed threshold values because ROC curves are obtained for a wide range of thresholds by plotting estimated true positive rates against false positive rates. In the present study, each univariate DSF is treated as a separate classifier of the healthy and damaged datasets. However, investigating each ROC is impractical for high dimensional DSFs. Thus, AUCs are adopted herein. They provide assessment of the classification performance as scalar values, where AUC=1.0 represents a perfect classification and a random classifier is characterised by AUC=0.5. Then, DSF rankings can be obtained by descend sorting of AUC values estimated for each univariate DSF.

2.4 Hierarchical adaptive neuro-fuzzy inference systems

The proposed methodology is based on the assumption that explicitly accounting for the differently distributed damage sensitivities in multivariate DSFs can lead to accurate damage

detection and severity estimation results with improved computational efficiency. Therefore, the HANFIS model structure is employed, as shown in Figure 1. The inputs refer to either the ranked univariate initial or secondary DSFs, v_i, where indices 1 and m correspond to the most and least sensitive univariate DSF, respectively. The squares are single ANFISs with two inputs and one output, where the outputs of lower level ANFISs propagate to higher levels. In general, fuzzy inference systems describe the relationship between inputs and outputs on the basis of fuzzy logic [10], which is numerically expressed by partial membership of an element in a set. Herein, the first-order Takagi-Sugeno fuzzy system is used, which can be represented as an ANN with five layers. In the first layer, the membership grades of inputs are calculated with non-linear membership functions. Gaussian membership functions are adopted in this study. Normalized firing strengths are then calculated in the second and third layer. The fourth layer evaluates fuzzy if-then rules with linear output membership functions. Finally, the ANFIS output is obtained by summation of the signals coming from previous layer. The number of input membership functions in each ANFIS is determined by unsupervised subtractive clustering of its raw inputs in order to account for their characteristics in different hierarchy levels.

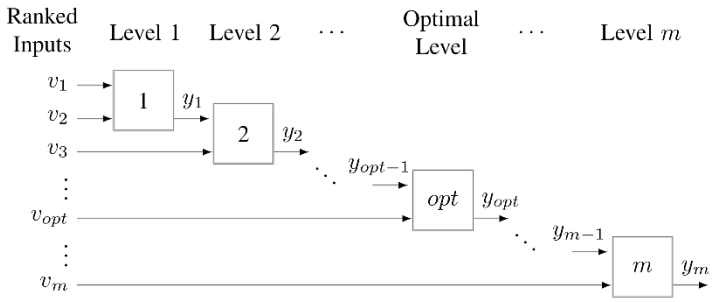

Figure 1: HANFIS structure.

Nonetheless, the single ANFISs are trained separately against desired outputs, i.e. damage severities in the present case, using root mean squared errors, ε_i, defined as:

$$\varepsilon_i = \sqrt{\sum_{j=1}^{n} \left(y_j - \hat{y}_{j,i} \right)^2} \tag{11}$$

where y_j are the true outputs and $\hat{y}_{j,i}$ the estimated outputs of the i-th ANFIS, respectively. The training is done with the help of a hybrid optimization [10], where the least squares estimation and gradient descent optimization are combined. Several epochs are evaluated iteratively. A hold-out cross-validation is applied to avoid overfitting. Here, a separate checking dataset is used to identify the optimal number of epochs, which is given by the smallest checking error.

A similar strategy is proposed for selecting the optimal number of HANFIS levels. However, this model identification task is considered as more complex, thus a k-fold cross-validation is used for investigating approximation and estimation errors of a certain model. Therefore, a model selection criterion, MSC_i, is defined in terms of the cross-validation error, $\bar{\varepsilon}_{cv,i}$, and the error standard deviation, $\sigma_{\varepsilon_{cv,i}}$, as:

$$\mathrm{MSC}_i = \bar{\varepsilon}_{cv,i} + \sigma_{\varepsilon_{cv,i}} \tag{12}$$

This allows selecting the HANFIS with an optimal (*opt*) layers of ANFISs using ranked univariate DSFs with the highest sensitivities down to v_{opt}.

3. EXPERIMENTS

For demonstrating the applicability of the proposed structural damage detection and severity estimation method, dynamic experiments with a small scale WTB are performed. The 2.36 m long WTB has a constant solid cross-section defined by the aerofoil E387 with a width of 150 mm. It is made by pultrusion of a glass-fibre reinforced epoxy composite material. The total mass of the WTB is measured as 7,110 g and the density is calculated with respect to the measured geometry as approximately 2.30 g/cm^3. To avoid self-weight effects, a vertical configuration is chosen for the experiments, as shown in Figure 2a. By attaching the WTB rigidly to a massive steel base, cantilever type boundary conditions are created. A household fan with a rotor diameter of 40.6 cm and an adjusted height of 62.0 cm measured from the WTB's root is used to apply contact-free excitations. Damage is introduced non-destructively by attaching small magnets of known masses at the WTB's trailing-edge approximately 30% of the WTB length from the root. This location is selected because it is prone to damage in large WTB as reported in inspection reports and damage studies [16,17].

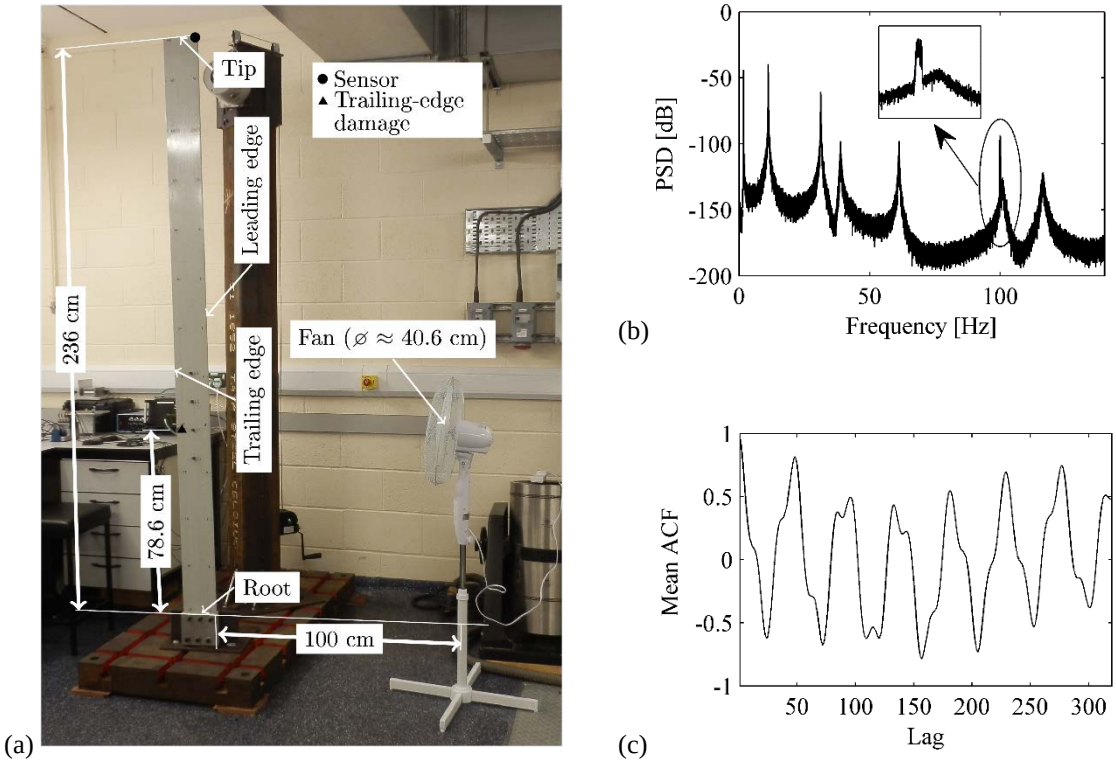

Figure 2: Dynamic WTB experiments: (a) experimental configuration, (b) PSD of flap-wise acceleration responses at the WTB's tip, (c) mean ACF estimated from one measurement of the healthy WTB.

In this study, only flap-wise vibrational responses at the WTB's tip are considered. They are measured with a single miniature piezoelectric accelerometer model Metra KS94B-100 with approximately 100 mV/g sensitivity and a frequency range between 0.5 Hz and 28 kHz. Data acquisition is done with a National Instruments (NI) data acquisition card model NI-9234 connected to an NI cDAQ-9174 chassis and laptop with NI's LabView software.

Figure 2b shows the power spectral density (PSD) for flap-wise accelerations measured at the tip of the healthy WTB excited with the fan. They are calculated using the Welch

estimator with eight 50% overlapping time series segments of a 30 min long reading at a sampling rate of 2048 Hz. It can be seen that the power of the signal decays significantly for higher frequency contents. Furthermore, only a few eigenmodes are excited, which appear as sharp peaks. From previous experimental modal analysis, they are identified as flap-wise bending modes at 1.75 Hz, 11.1 Hz, 31.3 Hz, 61.3 Hz, 100.8 Hz and torsional modes at 38.8 Hz and 116.1 Hz. These low frequencies are characteristic for the high flexibility of the WTB. However, a closer investigation of the spectrum at approximately 100 Hz reveals a spurious peak (see inset in Figure 2b), which is identified by further experiments as exogenous mechanical excitation. This excitation has non-stationary characteristics and cannot be controlled. Therefore, all signals are pre-processed for the following analysis with a discrete-time, equiripple, narrow stop-band, finite impulse response filter with the first and second stop band frequencies at 99.8 Hz and 100.1 Hz, respectively. The resulting delay is removed before signals are low-pass filtered using an eighth order Chebyshev Type I filter with a cut-off frequency of 409.6 Hz and resampled at 512 Hz. This sequential pre-processing is performed for all 30 min long readings of the healthy and damaged WTB. Then, each signal is divided into 400 segments of 5 s length with an overlap of approximately 10%, which are standardized with respect to their estimated means and standard deviations. Initial DSFs as ACFs with lags from 1 to 320 are calculated from each time series segment. Figure 2c shows the mean ACF estimated from a single measurement in the healthy state.

4. STRUCTURAL DAMAGE DETECTION AND SEVERITY ESTIMATION

The application of the proposed methodology for structural damage detection and severity estimation is presented in this section. First, the extraction of FKT scores and the damage sensitivity ranking of the initial and secondary DSFs is discussed. Then, optimal hierarchy levels of HANFISs for each DSF type are identified. Finally, both optimal HANFISs are compared with respect to their accuracy and computational costs.

4.1 Damage sensitive feature extraction and ranking

Secondary DSFs are extracted with the help of the FKT using three DSF matrices of the healthy state and one DSF matrix of the WTB with 40 g attached mass as the reference damage state. They are used to estimate first the normalizing matrix $\mathbf{P}$. However, the full eigendecomposition of the combined variance-covariance matrix, $\widehat{\mathbf{\Sigma}}$, leads to eigenvalues, λ_i, close to zero, see Figure 3a. These can cause numerical instabilities, thus only the 268 largest eigenvalues and corresponding eigenvectors are used to calculate $\mathbf{P}$ due to the significant decay for smaller eigenvalues. Then, the second eigenvector matrix, $\mathbf{\Phi}$, is computed, as discussed in Section 2.1.

The same matrices of initial DSFs are used for performing the univariate ranking, where secondary DSFs are obtained by transforming ACF-based DSFs. Figure 3b shows resulting AUCs of the ranked DSFs. It can be seen that the detectability of damage is differently distributed for both DSFs, where the first two FKT scores outperform ACF coefficients with respect to the highest AUCs. Nonetheless, they decay more quickly, thus initial DSFs with ranks 3 to 320 have higher AUCs then FKT scores with the same rank.

4.2 Hierarchical neuro-fuzzy modelling

Training soft-computing models for damage detection and severity estimation with sufficient resolution requires the use of additional datasets in contrast to the previous DSF ranking in order to learn the relationship between DSFs and structural states. Therefore, additional DSF

matrices are used with 20 g, 60 g, 80 g and 100 g masses attached to the WTB. Then, HANFIS models are trained for increasing numbers of hierarchy levels. Optimal levels are selected with respect to the introduced model selection criterion, MSC_i, by applying a five-fold cross-validation. Figure 4a shows the results for ACFs and FKT scores as DSFs. The criterion shows for the ACF HANFIS model a fast decrease until hierarchy level 25 and remains then almost constant. For the FKT HANFIS, a similar behaviour can be observed but generally with lower MSC_i values and as a less smooth function. Based on these observations, a hierarchy level of 25 is selected for both models and a final training is performed using all datasets for creating the final HANFISs. Nonetheless, Figure 4b shows the total numbers of model parameters, which are related to the models' computational complexity. A linear increase in the number of model parameters with increasing hierarchy levels can be seen for both HANFISs. However, the FKT HANFIS requires approximately 40% less parameters then the ACF HANFIS with the same hierarchy levels, which is a result of the adaptive subtractive clustering initialization of membership functions applied in each level and the better feature damage sensitivities.

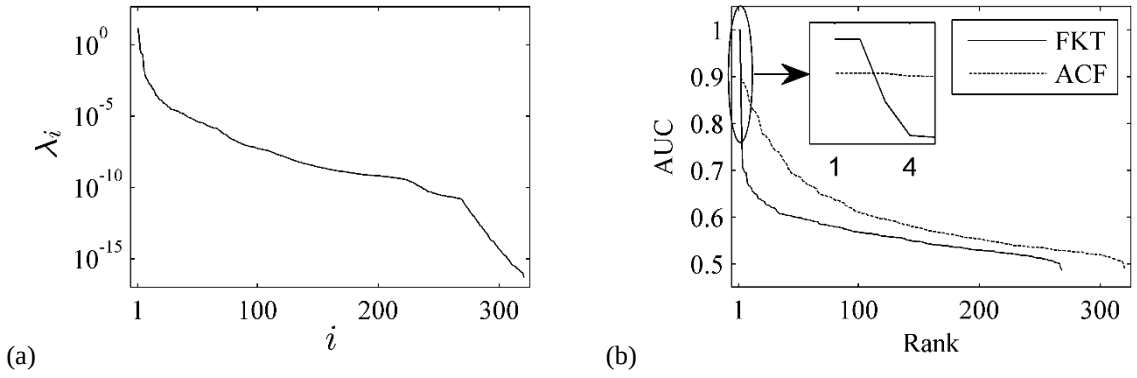

Figure 3: DSF extraction and ranking: (a) sorted eigenvalues of $\widehat{\boldsymbol{\Sigma}}$, (b) AUCs of ranked DSFs.

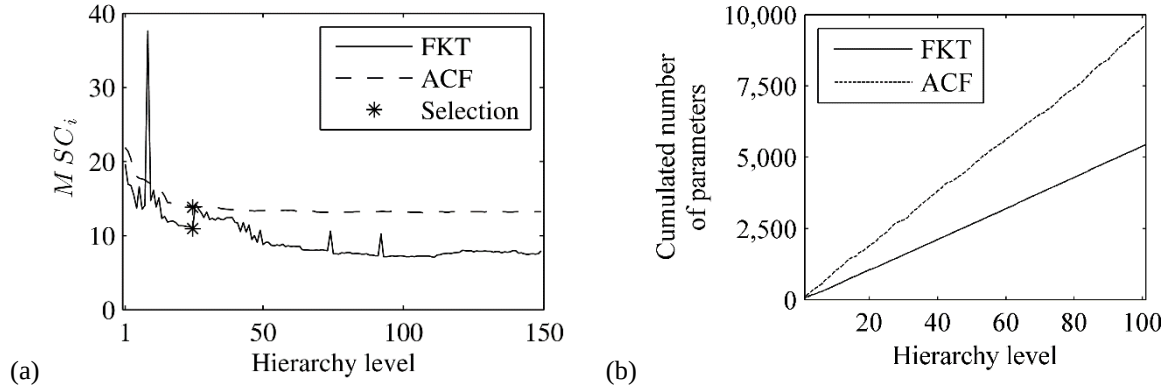

Figure 4: HANFIS modelling: (a) hierarchy level selection, (b) cumulated numbers of model parameters.

4.3 Structural damage detection and severity estimation results

Structural damage detection and severity estimation is performed using previously unseen datasets including damage extents not used for training. The results are shown in Figure 5, where the estimated masses are compared to the true masses attached. For each structural state, HANFIS outputs are analysed by grouping the data into 100 bins of constant widths and calculating relative frequencies for these bins. The FKT HANFIS leads to sharp

classifications of the damage extents in contrast to the ACF HANFIS, where outputs are significantly more blurred. Considering damage detection only, the FKT HANFIS does allow distinguishing between the healthy state and damage states with masses larger than 10 g, where it should be noted that the 10 g attached mass is a structural state outwith training state and including it in the training process may lead to better detectability. On the other hand, the less crisp outputs of the ACF HANFIS cause lower damage detectability results because states with less than 40 g are frequently indicated as healthy. It can be observed that both HANFIS models can estimate trained structural states with higher accuracy than untrained states. For the latter, the FKT HANFIS behaves like a classifier by assigning learned class labels to the new data. These classifications are close to the true structural states, e.g. samples of the WTB with 30 g attached mass are evenly classified as 20 g and 40 g. The ACF HANFIS outputs are more blurred with wider output ranges. For example, for the 30 g mass scenario, the outputs vary between 0 g and 40 g.

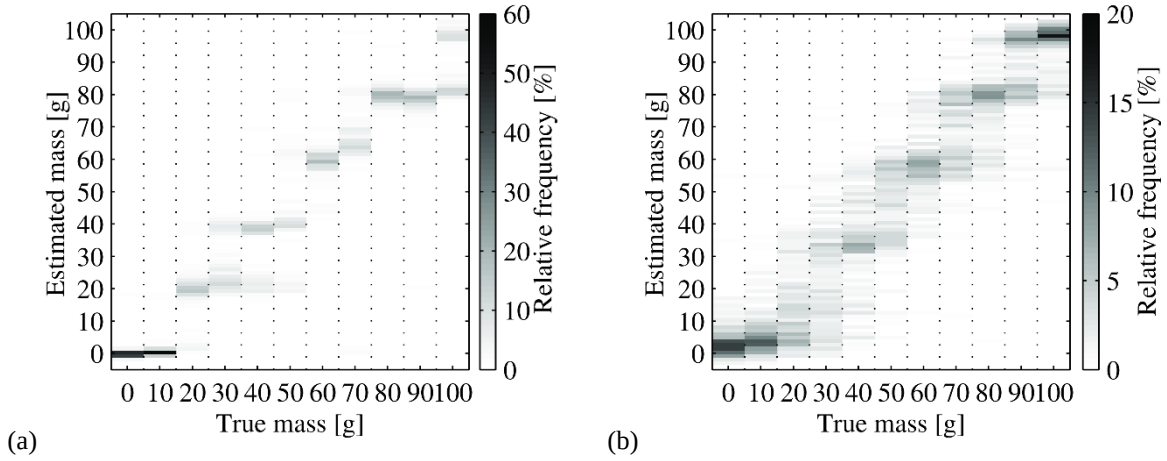

Figure 5: Structural damage detection and severity estimation results: (a) FKT HANFIS, (b) ACF HANFIS.

5. CONCLUSIONS

This study presents an application of a novel methodology for structural damage detection and severity estimation based on hierarchical neuro-fuzzy models and the FKT of vibration response correlations. The method is applied to experimental data of small scale WTB excited using a household fan, with damage simulated non-destructively by attaching small masses at the WTB's trailing-edge.

Hierarchical neuro-fuzzy models are developed under the assumption that DSFs are differently affected by damage and considering only those with the highest damage sensitivities can lead to better performance at lower computational cost. Therefore, two DSFs are studied. First, ACFs of acceleration responses are used as initial DSFs. Second, the FKT is performed to improve the damage sensitivity of initial DSFs. Then, a univariate ranking for both DSFs types is created with respect to the ability for distinguishing healthy and reference damage states. This ranking information is used for constructing hierarchical neuro-fuzzy models, where an optimal number of hierarchy levels is identified by cross-validation.

The potential of the proposed methodology for enhanced vibration-based SHM in WTBs is demonstrated. Hierarchical neuro-fuzzy models enable to detect damage and estimate its severity. Furthermore, the application of FKT for obtaining DSFs with improved damage sensitivity is found to be beneficial for the construction of these soft-computing models with respect to accuracy and computational efforts. This is promising for the

development of efficient SHM systems to be applied in real WTs in order to deliver higher safety and reliability at lower costs.

ACKNOWLEDGEMENTS

Piotr Omenzetter and Simon Hoell's work within the Lloyd's Register Foundation Centre for Safety and Reliability Engineering at the University of Aberdeen is supported by Lloyd's Register Foundation. The Foundation helps to protect life and property by supporting engineering-related education, public engagement and the application of research.

REFERENCES

[1] United Nations Framework Convention on Climate Change, "*Adoption of the Paris agreement"*, Draft decision -/CP.21, 1-32, (2015).
[2] Det Norske Veritas (DNV), *"Offshore standard: DNV-OS-J101"*, (2011).
[3] Lloyd's Register, *"Guidance on offshore wind farm certification"*, (2012).
[4] M.I. Blanco, The economics of wind energy, *Renewable and Sustainable Energy Reviews*, **13**, 1372-1382, (2009).
[5] P.J. Schubel, R.J. Crossley, E.K.G. Boateng, J.R. Hutchinson, Review of structural health and cure monitoring techniques for large wind turbine blades, *Renewable Energy*, **51**, 113-123, (2013).
[6] E.P. Carden, P. Fanning, Vibration based condition monitoring: A review, *Structutral Health Monitoring*, **3**, 355-377, (2004).
[7] S.D. Fassois, J.S. Sakellariou, Time-series methods for fault detection and identification in vibrating structures, *Philosophical Transactions of the Royal Society A: Mathematical, Physical and Engineering Sciences*, **365**, 411-448, (2007).
[8] O.R. de Lautour, P. Omenzetter, Damage classification and estimation in experimental structures using time series analysis and pattern recognition, *Mechanical Systems and Signal Processing*, **24,** 1556-1569, (2010).
[9] Y. Kim, J.W. Chong, K.H. Chon, J. Kim, Wavelet-based AR-SVM for health monitoring of smart structures, *Smart Materials and Structures*, **22**, 1-12, (2013).
[10] J.S.R. Jang, C.T. Sun, E. Mizutani, *"Neuro-Fuzzy and Soft Computing: A Computational Approach to Learning and Machine Intelligence"*, Prentice-Hall, Inc., Upper Saddle River, USA (1997).
[11] K. Fukunaga, W.L.G. Koontz, Application of the Karhunen-Loéve expansion to feature selection and ordering, *IEEE Transactions on Compututers*, **C-19**, 311-318, (1970).
[12] J.S. Bendat, A.G. Piersol, *"Random Data Analysis and Measurement Procedures"*, Fourth Edition, John Wiley & Sons, Inc., Hoboken, USA (2010).
[13] X. Huo, A statistical analysis of Fukunaga-Koontz transform, *IEEE Signal Processing Letters*, **11**, 123-126, (2004).
[14] S. Zhang, T. Sim, Discriminant subspace analysis: A Fukunaga-Koontz approach, *IEEE Transactions on Pattern Analysis and Machine Intelligence*, **29**, 1732-1745, (2007).
[15] W.J. Krzanowski, D.J. Hand, *"ROC Curves for Continuous Data"*, Taylor and Francis Group, LLC, Boca Raton, USA (2009).
[16] F.M. Jensen, A. Kling, J.D. Sørensen, Scale-up of wind turbine blades - changes in failure type, *Proceedings of EWEA Annual Event 2012*, Copenhagen, Denmark, 1-6, (2012).
[17] S. Ataya, M.M.Z. Ahmed, Damages of wind turbine blade trailing edge: Forms, location, and root causes, *Engineering Failure Analysis*, **35**, 480-488, (2013).